22. Nellis, W. J. *et al.*, *Phys. Rev. Lett.*, 1988, **60**, 1414.
23. Ahuja, R., Rekhi, S. and Johansson, B., *Phys. Rev.*, 2001, **B63**, 212101.
24. SESAME report on the Los Alamos Equation-of-state Library, LANL Report No. LALP-83-4, T-4 Group LANL, Los Alamos, 1983.
25. Mitchell, A. C. *et al.*, *J. Appl. Phys.*, 1991, **69**, 2981.
26. Evans, A. M., *et al.*, *Laser Particle Beams*, 1996, **14**, 113.
27. Kormer, S. B. *et al.*, *Sov. Phys. JETP*, 1962, **15**, 477.
28. Altshuler, L. V. *et al.*, *Sov. Phys. JETP*, 1962, **11**, 573.
29. Trunin, R. F. *et al.*, *Sov. Phys. JETP*, 1962, **29**, 630.
30. Marsh, S. P., *LASL Shock Hugoniot Data*, University of California Press, Berkeley, 1980.
31. Honrubia, J. J. *et al.*, *Advances in Laser Interaction with Matter and Inertial Fusion* (eds Velarde, G. *et al.*), World Scientific, Singapore, 1996, p. 34.

ACKNOWLEDGEMENTS. We acknowledge the encouragement and support received from Dr Anil Kakodkar. We are also extremely thankful to Dr S. K. Sikka, Dr D. D. Bhawalkar and Dr R. Chidambaram for their keen interest in the work and helpful discussions.

Received 17 February 2003; revised accepted 12 June 2003

Geochemistry of high-Mg mafic dykes from the Bastar craton: evidence of late Archaean boninite-like rocks in an intracratonic setting

Rajesh K. Srivastava* and R. K. Singh

Department of Geology, Igneous Petrology Laboratory, Banaras Hindu University, Varanasi 221 005, India

Mafic rocks of varying petrological and geochemical characteristics are exposed in the Bastar craton in the form of dykes as well as volcanics. Two sets of sub-alkaline mafic dyke swarms are well-recognized. The older set of sub-alkaline mafic dykes is middle Archaean, whereas the younger set is Palaeoproterozoic in age. In the present communication we report another set of mafic dyke swarms, which is also exposed in the southern part of the Bastar craton and has entirely different geochemical characteristics. This set of dyke swarms is intruded into granite gneisses and is late Archaean in age. Geochemically, these dykes contain high silica (> 52%) and magnesium (~ 12%) and low titanium (< 0.5%), classified as boninite. Phanerozoic boninitic rocks occur exclusively in convergent margin settings and are rarely seen in Precambrian terrains. In this respect, occurrence of such rocks in Bastar craton may have important tectonic implications. This communication presents preliminary results on petrological and geochemical characteristics of these high-Mg mafic dykes.

*For correspondence. (e-mail: rajeshgeolbhu@yahoo.com)

THE Archaean Bastar craton comprises a vast tract of granitoids and mafic rocks of different petrological characteristics, supracrustal rocks and unmetamorphosed late Proterozoic sedimentaries[1–3]. The Bastar craton is bounded by NW–SE trending Mahanadi and Godavari rifts, ENE–WSW trending Narmada–Son rift and Eastern Ghats Mobile Belt[2] (Figure 1). These rifts are supposed to be ancient and probably existed since the Archaean time[4,5]. Existence of these rifts in central Indian craton since the Archaean time and regional geology, including metamorphism[3] and distinctive sedimentary records[6,7], suggest the existence of a stable continental rift environment in the Central Indian craton[8–13].

Mafic igneous rocks of Precambrian age are a common feature that occurred in almost all the Archaean cratons of the globe, including the Indian Shield and provided valuable information on the role of crustal evolution[2,14–16]. The Archaean Bastar craton manifested several episodes of mafic magmatism, which include mafic dyke swarms and mafic volcanics[6,8–13]. Although few earlier workers have reported mafic dykes of different nature and age in this craton, little was known about their geochemical characteristics before the work done by the present authors. We have recognized two distinct mafic dyke swarms of sub-alkaline nature in the southern part of the Bastar craton[8,13]. The middle Archaean older set of sub-alkaline mafic dykes is metamorphosed under amphibolite facies conditions and shows low-Ti (~ 1.7%), low-Fe and moderate-Mg (~ 6%) geochemical characteristics. On the other hand, the younger set, of sub-alkaline mafic dykes which is Palaeoproterozoic (~ 1.8 Ga) in age, is fresh and shows comparatively different geochemical

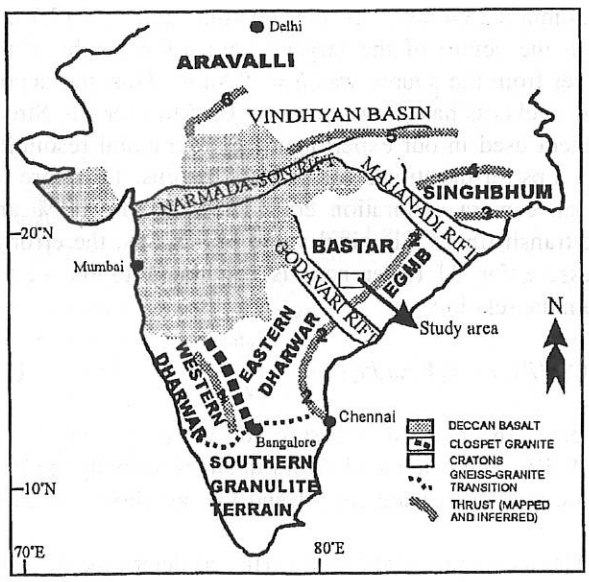

Figure 1. Major cratons and structural features of India[2]. Major structural features are: 1, Small thrusts in western Dharwar craton; 2, Eastern Ghats front; 3, Sukinda; 4, Singhbhum; 5, Son Valley, and 6. Great Boundary fault. EGMB, Eastern Ghats Mobile Belt.

characteristics–high-Ti (2.3%), high-Fe and low-Mg (~4.5%)[8,13]. The northern part of the Bastar craton comprises either high-Mg or high-Fe quartz tholeiite dykes emplaced in a sialic continental crust[9]. The mafic volcanic rocks are also well-exposed in the Bastar Craton[6,10–12]. Two generations of sub-alkaline basalts are reported from the Dongargarh area (the northern portion of the Bastar craton); early phases are emplaced during the late Archaean time and late phases show Proterozoic age[6], whereas the southern Bastar craton comprises geochemically diverse, well-exposed mafic volcanics emplaced during the late Archaean time[10–12]. Geochemically, southern Bastar mafic volcanic rocks are divided into three distinct varieties: sub-alkaline basalt, basaltic andesite, and boninite[12].

The present communication reports another set of mafic dyke swarms that shows entirely different petrological and geochemical characteristics, exposed in the southern Bastar craton. These dykes show important field observations: (i) they trend in NW–SE to WNW–ESE direction and are emplaced in the Archaean granite gneisses (3.6–2.6 Ga)[17], (ii) no dyke of this swarm is reported to cut the Proterozoic granites (2.3 Ga)[3], (iii) at one place a dyke of this swarm cuts a dyke of an older set of sub-alkaline mafic dyke swarm, and (iv) veins of younger granite (2.3 Ga) are reported to cut a dyke of this swarm[3]. These field observations clearly suggest their emplacement during the late Archaean time. These dykes are metamorphosed under greenschist facies conditions. They show either acicular or decussate texture and mainly consist of actinolite, chlorite, plagioclase (albite–oligoclase), epidote, quartz and iron oxides.

Out of several samples collected from the dykes of this set, ten fresh samples were selected for the whole rock major and trace-element analyses. Four of these samples were analysed for their rare-earth element concentrations (Table 1). All samples were analysed at Activation Laboratories, Ancaster, Canada by fusion inductively coupled plasma mass spectrometry. Several international geochemical reference material samples (STM1, MRG1, MAG1, BIR1, DNC1, and W2) were run along with these samples. Precision was approximately 5 and 5–10% for major oxides and trace/rare-earth elements, respectively.

Geochemical data show that these mafic dykes have high-silica (52.91–54.15 wt%), high-magnesium (10.91–16.19 wt%), and low-Ti (0.39–0.49 wt%) contents. These samples have been classified on the basis of their chemical compositions following recommendations of the IUGS sub-commission on Systematics of Igneous Rocks[18–20]. This chemical classification is based on the total alkalis and silica contents. According to IUGS recommendations, andesite/basaltic andesite and boninite rocks have similar silica and alkalis contents, but boninite samples have higher MgO (>8%) and lower TiO_2 (<0.5%) contents than adesites/basaltic andesites. Basaltic komatiites contain ≤50% silica with the same MgO content, observed in boninites. On this chemical classificatory diagram, all the studied samples are classified as boninite (Figure 2 *a*). These samples have also been classified on the basis of their normative compositions (Figure 2 *b*). Normative compositions are calculated assuming $FeO/(FeO + Fe_2O_3) = 0.85$. All samples fall at the hypersthene corner, which is designated for the boninitic rocks[21]. The IUGS sub-commission has not included some other high-Mg rocks such as norite and siliceous high-magnesium basalts (SHMB) in the chemical classification schemes[19,20]. Compared to boninite, these high-Mg rocks have relatively lower SiO_2 and higher TiO_2 contents, although it is not easy to distinguish boninites from the norite and SHMB samples on the basis of limited geochemical data.

To observe further geochemical characteristics of the studied high-Mg dyke samples, primordial mantle-normalized multi-element and chondrite-normalized rare-earth element patterns are presented (Figure 3). From these patterns it is observed that all the plotted elements show enriched concentrations than the primordial mantle and the chondrite values. The large-ion lithophile ele-

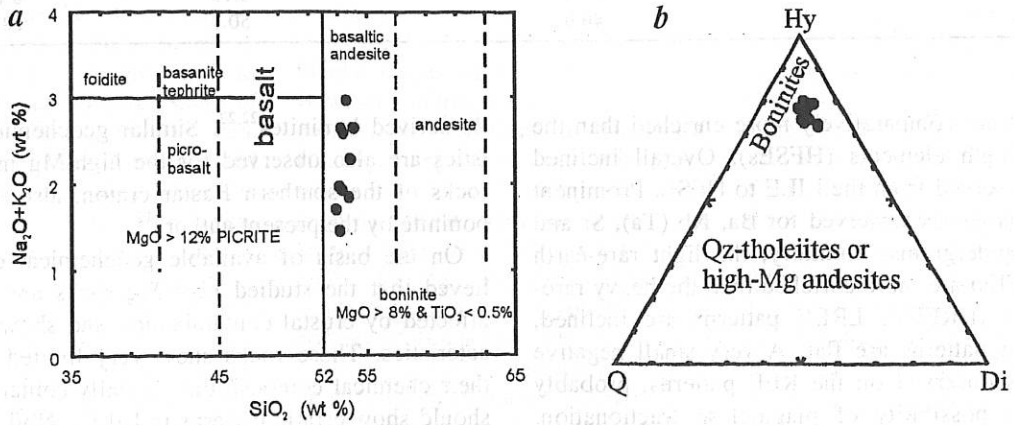

Figure 2. *a*, Total alkalis-silica (TAS) diagram for high-Mg volcanic rocks[19,20]; *b*, CIPW normative classification[21].

Table 1. Whole rock major (wt% oxides), trace and rare-earth elements (in ppm) analyses of high-Mg dykes from the southern Bastar Craton, Central India

Sample no. →	1 97/175	2 97/185	3 97/198	4 97/207	5 97/210	6 97/303	7 97/340	8 97/369	9 97/378	10 97/381
SiO_2	53.65	53.34	53.42	53.81	53.92	54.15	53.19	53.25	53.14	52.91
TiO_2	0.49	0.46	0.49	0.41	0.46	0.48	0.39	0.48	0.43	0.39
Al_2O_3	12.35	10.69	11.24	9.60	10.85	11.37	8.90	10.69	10.92	10.25
Fe_2O_3	11.08	10.62	11.02	10.90	10.76	11.18	11.13	11.72	10.50	10.31
MnO	0.18	0.17	0.18	0.18	0.17	0.17	0.18	0.19	0.17	0.18
MgO	10.91	12.80	11.94	15.36	12.84	12.01	16.19	13.05	13.30	14.59
CaO	6.83	6.37	6.25	5.60	6.24	6.72	5.82	5.83	6.11	6.25
Na_2O	1.65	1.41	1.44	1.05	0.93	1.68	0.97	1.46	1.12	1.05
K_2O	1.31	0.51	1.14	0.79	1.35	0.96	0.48	1.17	0.84	0.65
P_2O_5	0.06	0.07	0.07	0.06	0.06	0.07	0.05	0.07	0.12	0.05
Total	98.51	96.44	97.19	97.76	97.58	98.79	97.30	97.91	96.65	96.63
LOI	2.13	3.48	1.79	2.46	2.62	1.84	1.90	2.18	3.22	1.90
$Mg^{\#}$	66.10	70.47	68.21	73.62	70.27	68.02	74.23	68.80	71.50	73.70
Cr	–	–	–	1500	–	–	1590	–	927	1080
Ni	–	–	–	361	–	–	365	–	310	278
Sc	31	30	31	31	30	30	28	32	31	30
V	173	173	179	173	174	168	150	184	170	167
Rb	–	–	–	43	–	–	27	–	47	32
Ba	311	138	236	138	186	267	152	194	205	139
Sr	96	91	109	67	63	81	85	62	70	65
Ga	–	–	–	5	–	–	5	–	7	5
Ta	–	–	–	0.52	–	–	0.33	–	0.32	0.32
Nb	–	–	–	3.0	–	–	3.0	–	3.0	3.0
Hf	–	–	–	1.60	–	–	1.60	–	1.60	1.50
Zr	66	64	70	56	64	71	58	65	58	54
Y	13	13	13	11	12	15	11	13	11	10
Th	–	–	–	4.30	–	–	4.30	–	4.30	4.10
La	–	–	–	9.40	–	–	9.70	–	9.30	9.40
Ce	–	–	–	20.00	–	–	19.00	–	21.00	19.00
Pr	–	–	–	2.16	–	–	2.01	–	2.06	2.09
Nd	–	–	–	8.30	–	–	8.00	–	8.10	7.90
Sm	–	–	–	1.70	–	–	1.70	–	1.80	1.80
Eu	–	–	–	0.47	–	–	0.48	–	0.52	0.47
Gd	–	–	–	2.00	–		1.80	–	2.00	1.90
Tb	–	–	–	0.30	–	–	0.30	–	0.30	0.30
Dy	–	–	–	2.00	–	–	2.00	–	2.10	1.80
Ho	–	–	–	0.40	–	–	0.40	–	0.40	0.40
Er	–	–	–	1.30	–	–	1.20	–	1.30	1.20
Tm	–	–	–	0.20	–	–	0.18	–	0.20	0.18
Yb	–	–	–	1.20	–	–	1.30	–	1.30	1.20
Lu	–	–	–	0.19	–	–	0.18	–	0.20	0.19
Nb/La				0.32			0.31		0.32	0.32
Nb/Ce				0.15			0.16		0.14	0.16
Ba/Nb				46.0			50.7		68.3	46.3

ments (LILEs) are comparatively more enriched than the high-field strength elements (HFSEs). Overall inclined patterns are observed from the LILE to HFSE. Prominent negative anomalies are observed for Ba, Nb (Ta), Sr and Ti on these spidergrams. Similarly, the light rare-earth elements (LREEs) are more enriched than the heavy rare-earth elements (HREEs). LREE patterns are inclined, whereas HREE patterns are flat. A very small negative Eu anomaly is observed on the REE patterns, probably precluding the possibility of plagioclase fractionation. The inclined LREE patterns are reported from the mantle-derived boninites[22,23]. Similar geochemical characteristics are also observed for the high-Mg mafic volcanic rocks of the southern Bastar craton, also recognized as boninite by the present authors[12].

On the basis of available geochemical data it is believed that the studied high-Mg rocks are probably not affected by crustal contamination and show source characteristics. These rocks show very limited variations in their chemical composition; crustally contaminated rocks should show erratic patterns in LILEs. Nb/La, Nb/Ce and Ba/Nb ratios also discourage the possibility of any crustal

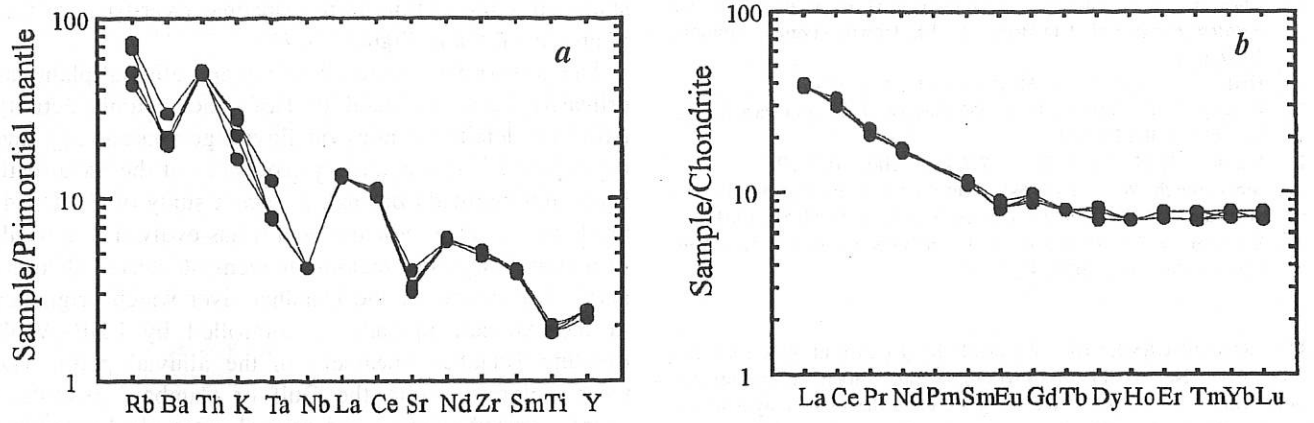

Figure 3. *a*, Primordial mantle-normalized[28] multi-element, and *b*, Chondrite-normalized[29] rare-earth element patterns for high-Mg dykes.

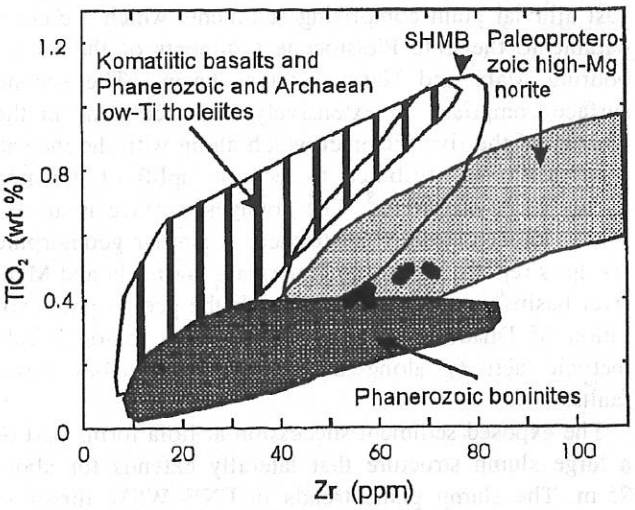

Figure 4. TiO_2–Zr diagram[23,27] showing different fields of high-Mg mafic rocks.

contamination. To fully rule out the possibility of crustal contamination, radioactive isotope data would be required. Figure 4 shows TiO_2 and Zr variations in common high-Mg and low-Ti mafic rocks. The studied samples show good correlation with boninite, SHMB and Palaeoproterozoic norite. Few samples clearly fall in the boninite field, but possibilities of other high-Mg derivatives cannot be discarded. Further geochemical and isotopic studies are required to confirm the existence of boninite in the Central Indian craton.

On the basis of the presented geochemical characteristics, it is concluded that the high-Mg mafic dykes encountered in the southern Bastar craton show boninite-like geochemical nature. Although most of the boninites occur in subduction zones, their occurrences in rift or continental environments are also well-reported by several researchers[24–27]. Further study of these rocks is recommended in view of the genesis of boninitic magma, because their existence may have important tectonic implications.

1. Crookshank, H., *Geology of Southern Bastar and Jeypore from the Bailadila to the Eastern Ghats*, Geol. Surv. India Mem., 1963, **87**, p. 150.
2. Naqvi, S. M. and Rogers, J. J. W., *Precambrian Geology of India*, Oxford Univ. Press, 1987, p. 233.
3. Ramakrishnan, M., *Geol. Surv. India Spec. Publ.*, 1990, **28**, 44.
4. Naqvi, S. M., Divakar Rao, V. and Narain, H., *Precambrian Res.*, 1974, **1**, 345.
5. Chaudhuri, A. K., Saha, D., Deb, G. K., Deb, S. P., Mukherjee, M. K. and Ghosh, G., *Gondwana Res.*, 2002, **5**, 23.
6. Neogi, S., Miura, H. and Hariya, Y., *Precambrian Res.*, 1996, **76**, 77.
7. Radhakrishna, B. P. and Naqvi, S. M., *J. Geol.*, 1986, **94**, 145.
8. Srivastava, R. K., Hall, R. P., Verma, R. and Singh, R. K., *J. Geol. Soc. India*, 1996, **48**, 537.
9. Ramachandra, H. M., Mishra, V. P. and Deshmukh, S. S., in *Dyke Swarms of Peninsular India* (ed. Devaraju, T. C.), Geol. Soc. India Mem., 1995, 33, p. 183.
10. Srivastava, R. K. and Singh, R. K., *J. Geol. Soc. India*, 1999, **53**, 693.
11. Srivastava, R. K. and Singh, R. K., *AGSO-Geosci. Aust. Rec.*, 2001, **37**, 196.
12. Srivastava, R. K., Singh, R. K. and Verma, S. P., *Precambrian Res.*, 2004 (in press).
13. Srivastava, R. K. and Singh, R. K., *J. Asian Earth Sci.*, 2003 (in press).
14. Hall, R. P. and Hughes, D. J. (eds), *Early Precambrian Basic Magmatism*, Blackie, London, 1990, p. 486.
15. Weaver, B. L., see ref. 14, p. 339.
16. Smith, T. E., in *Proterozoic Crustal Evolution* (ed. Condie, K. C.), Elsevier, Amsterdam, 1992, p. 7.
17. Sarkar, A., Sarkar, G., Paul, D. K. and Mitra, N. D., *Geol. Surv. India Spec. Publ.*, 1990, **28**, 453.
18. Le Bas, M. J., Le Maitre, R. W., Streckeisen, A. and Zanettin, B., *J. Petrol.*, 1986, **27**, 745.
19. Le Bas, M. J., *J. Petrol.*, 2000, **41**, 1467.
20. Le Maitre, R. W., *Igneous Rocks: A Classification and Glossary of Terms*, Cambridge Univ. Press, 2002, p. 236.
21. Thompson, R. N., *Proc. Geol. Assoc.*, 1984, **95**, 249.
22. Cameron, W. E., McCulloch, M. T. and Walker, D. A., *Earth Planet. Sci. Lett.*, 1984, **65**, 75.
23. Poidevin, J. L., *Precambrian Res.*, 1994, **68**, 97.

24. Crawford, A. J., Falloon, T. J. and Green, D. H., in *Boninites and Related Rocks* (ed. Crawford, A. J.), Unwin Hyman, London, 1989, p. 1.
25. Hatton, C. J. and Sharpe, M. R., see ref. 24, p. 174.
26. Piercey, S. J., Murphy, D. C., Mortensen, J. K. and Paradis, S., *Geology*, 2001, **29**, 731.
27. Smithies, R. H., *Earth Planet. Sci. Lett.*, 2002, **197**, 19.
28. McDonough, W. F., Sun, S-S., Ringwood, A. E., Jagoutz, E. and Hofmann, A. W., *Geochim. Cosmochim. Acta*, 1992, **56**, 1001.
29. Evensen, N. M., Hamilton, P. J. and O'Nion, R. K., *Geochim. Cosmochim. Acta*, 1978, **42**, 1199.

ACKNOWLEDGEMENTS. We thank the Department of Science and Technology, New Delhi for providing research grant for the present work (ESS/CA/A9-40/95). We are grateful to the two anonymous reviewers for their constructive comments which improved the earlier version of this manuscript considerably. R.K.S. also acknowledges CSIR for financial assistance as Senior Research Fellow.

Received 4 January 2003; revised accepted 20 May 2003

Evidence of a Mid–Late Holocene seismic event from Dhadhar river basin, Gujarat alluvial plain, western India

Rachna Raj*, N. Mulchandani, S. Bhandari, D. M. Maurya and L. S. Chamyal

Department of Geology, M. S. University of Baroda, Vadodara 390 002, India

Soft-sediment deformation structures have developed in a major slump at Itola in the Dhadhar river basin of Gujarat alluvial plain. The slump plane parallels the active Dhadhar lineament. Pseudonodules, pinching and folding, convolute folds, concave-up paths, clay diapirs, flamed convolutions and minor faults are the major deformational structures identified. Radiocarbon dating of an associated charcoal layer has given a maximum age of 5570 ± 30 yr BP. The soft-sediment deformation structures conform to the criteria for attributing them to a seismic event during Mid–Late Holocene.

RECOGNITION of past seismic events is important for understanding the seismic phenomena in areas experiencing earthquakes, such as western India. Soft-sediment deformation structures formed during or shortly after deposition of horizontal sedimentary layers in Quaternary geological records are important indicators of past seismic activity[1–5]. We report here soft-sediment deformation structures developed in the sediments of a large slump structure at Itola in the Dhadhar river basin of Gujarat alluvial plain (Figure 1 *a*, *b*).

The geomorphic evolution of Gujarat alluvial plain has primarily been attributed to Holocene tectonic activity based on detailed studies on fluvial geomorphology and the exposed Late Quaternary sequences of the Sabarmati, Mahi and Narmada basins[6]. A recent study of the Dhadhar basin has also indicated that it has evolved as a result of regional phases of tectonic movements during Quaternary[7]. The course of the Dhadhar river which originates in the Aravalli uplands is controlled by ENE–WSW trending Dhadhar lineament in the alluvial plain. The river, before meeting the Gulf of Cambay, exhibits a deeply incised channel and several entrenched meanders all along its course in the Gujarat alluvial plain. Three distinct geomorphic surfaces have been observed in the Dhadhar valley[7] (Figure 1 *b*). The oldest surface is the vast alluvial plain comprising sediments which are comparable to the Late Pleistocene sediments of the neighbouring Mahi and Narmada river basins. The second surface comprises an extensively dissected zone in the vicinity of the river channel which along with the incised cliffs has been attributed to tectonic uplift of the area during Early Holocene[8]. The youngest surface is an uplifted Holocene valley fill terrace. A similar geomorphic set up is reported from the Sabarmati, Narmada and Mahi river basins[6,8], which points towards the geomorphic evolution of Dhadhar valley in response to regional-scale tectonic activity along the subsurface Cambay basin faults.

The exposed sediment succession at Itola forms part of a large slump structure that laterally extends for about 25 m. The slump plane trends in ENE–WSW direction which is parallel to the Dhadhar lineament (Figure 1 *b*). The exposed sediment succession is about 6 m thick and consists of several horizons of sands, silts and clays with thin layers of charcoal (Figure 1 *c*). Soft-sediment deformational features are observed mainly within the silt and clay horizons intercalated with thin layers of terrigenous charcoal. Radiocarbon dating of a charcoal sample from this horizon (Figure 1 *c*) gave an age of 5570 ± 30 yr BP.

The various soft-sediment deformation structures identified include pseudonodules, pinching and folding, minor faulting, contorted structures which include convolute folds, concave-up paths, and intruded structures like clay diapirs, flamed convolutions, isolated flamed structures and sand dykes. The pseudonodules observed are of different morphologies consisting of isolated masses of sands present in the clayey deposits (Figure 2 *a*). The pseudonodules are generally irregular and resemble drop and sag-type structures described by Steward[9]. The formation of sand nodules by shaking effect has been experimentally proved by Kuenen[10], who simulated the deformational behaviour of sand overlying the clay. The formation of sand nodules in the area can be explained in

*For correspondence. (e-mail: naveenrachna@indiatimes.com)